Experimental and Theoretical Evidence for Ferromagnetic Edge in WSe_2 Nanosheets

Lei Tao[a⊥], Fanchen Meng[b⊥], Shudong Zhao[a], Yongli Song[a], Jianxin Yu[c], Xianjie Wang[a], Zhiguo Liu[a], Yi Wang[d], Bingsheng Li[b], Yang Wang[d*], Yu Sui[a*]

[a]Department of Physics, Harbin Institute of Technology, Harbin, People's Republic of China.

[b]Department of Physics and Astronomy, Clemson University, Clemson, SC, USA

[c]Center for Analysis and Measurement, Harbin Institute of Technology, Harbin, People's Republic of China

[d]Academy of Fundamental and Interdisciplinary Sciences, Harbin Institute of Technology, Harbin, People's Republic of China

Email: yangwang@hit.edu.cn and suiyu@hit.edu.cn

Keywords: WSe_2 nanosheets, ferromagnetism, density functional theory, chemical vapor deposition

Electronic Supplement Materials

Schematic Diagram of CVD Deposition

CVD system contains a single zone tube furnace whose diameter is 5 cm, a mechanical pump and a gas control system. The growth process was conducted under non-equilibrium state at low temperature to obtain WSe_2 nanosheets. As shown in Fig. S1, SiO_2/Si substrate was put on top of WO_3 powder.

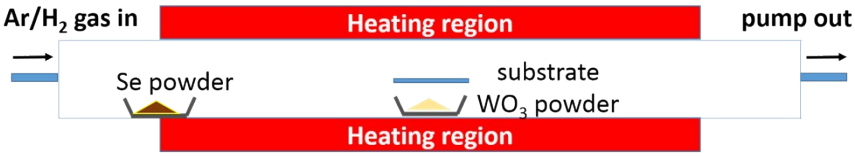

Fig. S1. Schematic diagram of CVD deposition in this experiment

Raman and PL characterization of edge regions in WSe_2 nanosheets

Edge regions of nanosheets in different shapes are characterized by Raman and photoluminescence (PL) measurements. Fig. S2a, b and c show optical images of three triangular WSe_2 nanosheets on SiO_2/Si substrate with small differences in shape of domains. PL spectrum is sensitive to local chemical and physical environment of material, thus it can be used to characterize defects, thickness, strain and exciton/trions in two dimensional materials, and the diameter of focused laser is about 1 μm which makes PL measurement suitable to characterize different parts of nanosheets.[1-4] In order to figure out the differences in edges among three triangular WSe_2 nanosheets, PL measurements were taken at three points marked as A, B and C in Fig. S2a along dashed line from central part to edge of nanosheets. Fig. S2b depicts the PL spectra of WSe_2 with different corner shapes. From center to edge, PL

spectrum of R-WSe_2 and S-WSe_2 experience a small blueshift (9 meV) and large blueshift (33 meV), respectively; while there is no significant frequency shift in F-WSe_2. Several reasons can influence PL peak of transition metal dichalcogenides (TMDCs), such as strain, temperature and size effect.[5,6] In this work, peak shifts in edges of different nanosheets is affected by change of local strain environment caused by structural construction, which consists with conclusion of following Raman data. Similar blueshift of PL spectrum of PL has been reported, where strain was applied on sample by stretching nanosheet causing structural construction[3]. The different blueshift in PL spectra of three WSe_2 nanosheets (Fig. S2b) indicates the edges of the three nanosheets structural different.

Raman measurements were taken at center and edge parts of nanosheets after PL measurements. WSe_2 monolayer consisting of three atom layers have various edge terminations, therefore curved edge and corner might show up. The outmost atoms could form many different kinds of coordination different from trigonal prismatic coordination at inner part of nanosheets, causing structure reconstruction at the edge.[7] Theoretical research has found chemical potential and growth rate play a dominant role in controlling shape and edge structures of nanosheets.[8] Compared with inner atoms, unsaturated edge atoms with dangling bonds and different coordination break the symmetry of crystal at the edge resulting in the appearance of new peak in Raman spectra. Fig. S2c shows normalized Raman spectra of R-WSe_2, F-WSe_2 and S-WSe_2 at three points (A, B and C) in a line from inner part to the edge of the nanosheets (Fig. S2a). Two typical peaks appeared at 250 cm^{-1} and 260 cm^{-1} corresponding to in-

plane E_{2g}^1 and out-of-plane A_{1g} vibrations. There is no significant difference between Raman spectra of edge and center position in all WSe_2 nanosheets, excepting that new peak at 308 cm^{-1} shows up in R-WSe_2 and F-WSe_2, which is ascribed to B_{2g}^1.[9] Appearance of new Raman peak and blue shifting of PL spectrum at the edge of nanosheets indicate CVD-grown WSe_2 nanosheets having different edge structures.

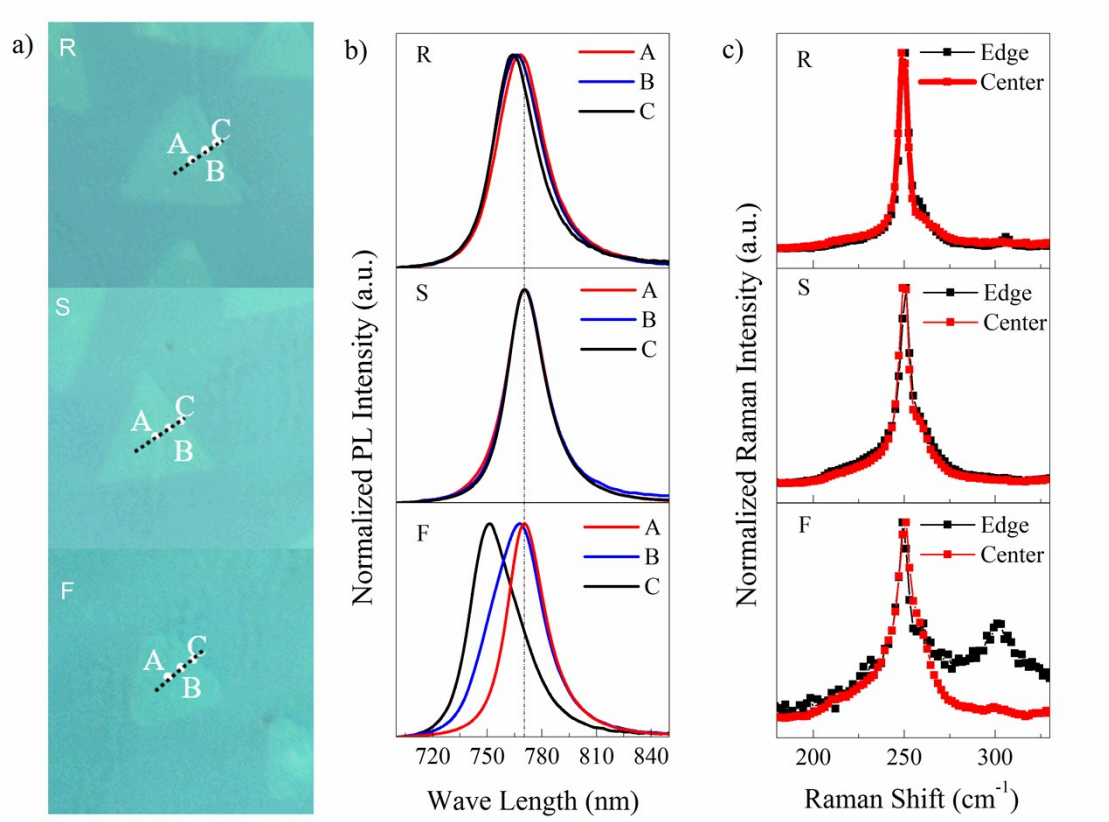

Fig. S2. (a) Optical images of WSe_2 nanosheets with round corner (R), sharp corner (S) and flat corner (F); (b) Raman spectra of R- WSe_2, S- WSe_2, F-WSe_2 nanosheets (c) PL spectra of R- WSe_2, S- WSe_2, F-WSe_2 nanosheets.

Raman mapping of WSe_2 at 250 cm^{-1} was also measured to observe potential defects at the edge of nanosheet. The Raman mapping image of the WSe_2 nanosheets was shown in Fig. S3, which shows a uniform feature. As a result, no obvious defects

were found near the edge of the WSe_2 nanosheet indicating high quality of the nanosheet.

Fig. S3 Raman mapping image of the WSe_2 nanosheet at the peak of 250 cm^{-1} (corresponding to the A_{1g} and E^1_{2g})

Calculation Details

We first optimized the geometry of monolayer WSe_2 with a k-point mesh of 9×9. As shown in Fig. 4a, the calculated lattice constants are a = b = 3.33 Å, which agree well with the experimental data 3.28 Å.[10] In addition, the band gap obtained in this calculation is 1.74 eV, which is also near the experimental value 1.75 eV obtained under 4 K.[11] Therefore, the choice of the calculation methods here is reasonable. It is interesting to note that even with spin-polarized calculation, no magnetic moment is found on monolayer WSe_2. With the calculated geometry of monolayer WSe_2, we are able to cut out the triangular WSe_2 clusters and zigzag nanoribbons. While in the calculation of zigzag WSe_2 nanoribbons, the one-dimensional lattice constant is kept fixed at 3.33 Å and k-space sampling remains 11 for all the nanoribbons calculated in this work. In the calculation of WSe_2 clusters, only gamma point is used for the k-space sampling.

Phase Shift of MFM Measurement

We adopted dynamic MFM measurement that recorded shift of resonant phase of resonant system consisting of cantilever and sample, and obtained MFM phase image with the tip lifted 20 nm up. Phase shift of cantilever reflected magnitude of magnetic force, termed as:

$$\Delta\phi \approx \frac{Q}{k}\frac{\partial F}{\partial z} \qquad (1)$$

Where Q is the quantity factor of vibration system, K is the elastic constant of cantilever, F is magnetic force between magnetic tip and sample, and z stands for the direction perpendicular to sample surface. Magnetic interaction between sample and magnetic tip can cause phase shift of cantilever. If the interaction between the tip and sample is stronger, displacement of cantilever along z-direction will be bigger leading to a larger phase shift.

Effect of thickness, substrate and electrostatic force on magnetism

In order to investigate how thickness influences magnetic moment at the edge of nanosheets, MFM measurement of multi-layer WSe_2 nanosheet was also carried out. Magnetic edge is also found in multi-layer WSe_2 nanosheets. Fig. S4a show AFM image of WS_{e2} nanosheets with multi-layers on its edge and center. The step edge of nanosheet mainly consists of two parts: a 4.3 nm (6 atom layers) thick bottom layer and a 1.8 nm (2 atom layers) thick top layer as shown in Fig. S4c. Combining the MFM phase profile (Fig. S4d) and its AFM height profile (Fig. S4c), the 4.3 nm thick edge has no significant MFM phase shift compared with nonmagnetic substrate. But maximum phase shift appeared at the 1.8 nm thick top layer corresponding to the

region from 1 μm to 1.5 μm. The results show that thicker nanosheets had a smaller phase shift indicating magnetic interaction between edge of nanosheets and magnetic tip decrease as thickness of nanosheets increase. As the result of our theoretical calculation, magnetic moment presents the edge of WSe_2 cluster indicating that the magnetic state is edge state. Precious studies show that edge states are sensitive to the thickness of the system due to surface effect and quantum confinement effect[12,13], the combination of the unsaturated electrons from Se and W atoms at the edge depends sensitively on layer thickness. Similar thickness dependent property, such as Raman and PL, were also found in other 2D TMDCs.[14] As a result, magnetic edge of WSe_2 nanosheets was influenced by quantum confinement effect and surface effect. The magnitude of magnetic moment increase as the number of layer decreases. When the layer number of the nanosheet exceeds 6 layers, magnetic edge of the nanosheet disappears and the nanosheet exhibits magnetic behavior as same as WSe_2 in bulk form.

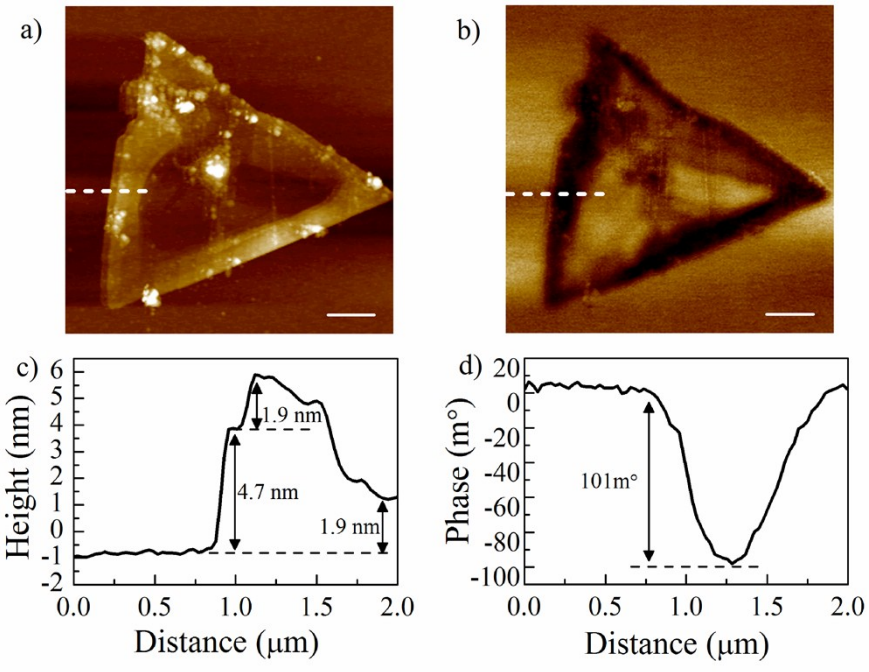

Fig. S4 (a) AFM image and (b) MFM phase image of multi-layer WSe_2 nanosheets. Their corresponding profiles along dashed lines in panels (a) and (b) are shown in panels (c) and (d), respectively. The scale bar is 1 μm.

The bottom-up grown WSe_2 nanosheets have a weak Van der Waals interaction with substrate. Although the force between substrate and nanosheets is weak, the interface can influence the properties of nanosheets, such as substrate influences PL property of nanosheets by doping electrons or holes in nanosheets.[6] In order to test whether magnetic edge of WSe_2 nanosheets originates from interface effect or not, MFM phase of WSe_2 nanosheets on Si substrate was measured. Fig. S5 shows the AFM and MFM phase image of WSe_2 nanosheet on Si substrate, a clear magnetic edge was also found, which is similar as nanosheets grown on SiO_2/Si substrate, indicating that interface has no impact on magnetic edge of nanosheets.

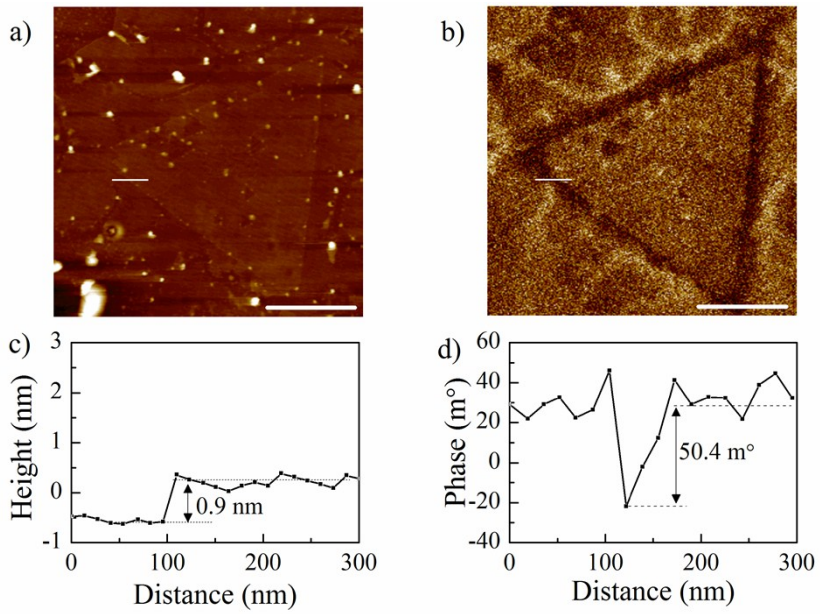

Fig. S5 (a) AFM image and (b) MFM phase image of WSe_2 monolayer. Their corresponding profiles along short lines in panels (a) and (b) are shown in panels (c) and (d), respectively. The scale bar is 1 μm.

Electrostatic force between sample and MFM tip may also influence results of MFM measurements. To provide reliable MFM results, MFM measurements of the same nanosheet were taken under different bias voltages shown in Fig. S6. No obvious phase change was observed under different bias voltages, indicating that the electrostatic force has little impact on MFM measurement of sample.

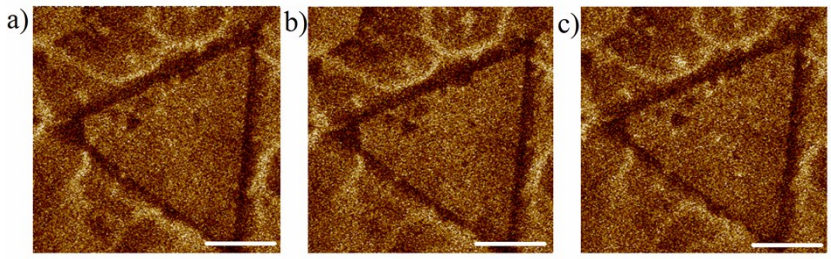

Fig. S6 MFM phase images of WSe_2 measured under different biased voltage, (a) 0 V, (b) 5 V and (c) -5 V. The scale bars are all 1 μm.

If bond between hydrogen and selenium was formed at the edges, the vibration modes of H-Se at 124 cm^{-1} and 331 cm^{-1} [15] could be observed in the Raman spectrum. Raman measurements were adopted to observe H-Se bond. As the Raman spectra at the edges shown in Fig. S7, there are no obvious peaks at 124 cm^{-1} or 331 cm^{-1} indicating no H-Se bonds are formed in our samples.

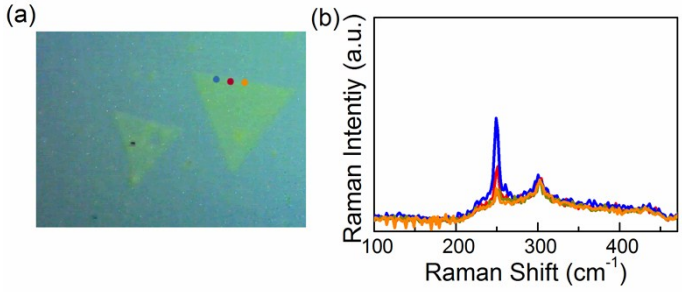

Fig. S7 (a) optical image of three points at the edge. (b) Raman spectra of WSe_2 nanosheet at the three points.

References

[1] Jiang, J., Pachter, R., Mehmood, F., Islam, A. E., Maruyama, B., Boeckl and J. J. (2015). A Raman spectroscopy signature for characterizing defective single-layer graphene: Defect-induced I (D)/I (D′) intensity ratio by theoretical analysis. Carbon, 90, 53-62.

[2] Berkdemir, A., Gutiérrez, H. R., Botello-Méndez, A. R., Perea-López, N., Elías, A. L., Chia, C. I. and Terrones, H. (2013). Identification of individual and few layers of WS_2 using Raman Spectroscopy. Scientific Reports, 3, 1755

[3] Desai, S. B., Seol, G., Kang, J. S., Fang, H., Battaglia, C., Kapadia, R. and Javey, A. (2014). Strain-induced indirect to direct bandgap transition in multilayer WSe_2. Nano Letters, 14(8), 4592-4597.

[4] Liu, B., Zhao, W., Ding, Z., Verzhbitskiy, I., Li, L., Lu, J. and Loh, K. P. (2016). Engineering Bandgaps of Monolayer MoS_2 and WS_2 on Fluoropolymer Substrates by Electrostatically Tuned Many‐Body Effects. Advanced Materials, 28(30), 6457-6464.

[5] Brothers, A. D. and Brungardt, J. B. (1979). Excitons in WS_2 films pressure and temperature effects. Physica Status Solidi (b), 91(2), 675-679.

[6] Frey, G. L., Tenne, R., Matthews, M. J., Dresselhaus, M. S. and Dresselhaus, G. (1998). Optical properties of MS_2 (M= Mo, W) inorganic fullerenelike and

nanotube material optical absorption and resonance Raman measurements. Journal of Materials Research, 13(09), 2412-2417.

[7] Liu, B., Fathi, M., Chen, L., Abbas, A., Ma, Y., Zhou, C. (2015). Chemical vapor deposition growth of monolayer WSe_2 with tunable device characteristics and growth mechanism study. ACS Nano, 9(6), 6119-6127.

[8] Zhu, S. and Wang, Q. (2015). A simple method for understanding the triangular growth patterns of transition metal dichalcogenide sheets. AIP Advances, 5(10), 107105.

[9] Luo, X., Zhao, Y., Zhang, J., Toh, M., Kloc, C., Xiong, Q., Quek and S. Y. (2013). Effects of lower symmetry and dimensionality on Raman spectra in two-dimensional WSe_2. Physical Review B, 88(19), 195313.

[10] Huang, C., Wu, S., Sanchez, A. M., Peters, J. J., Beanland, R., Ross, J. S. and Xu, X. (2014). Lateral heterojunctions within monolayer $MoSe_2$–WSe_2 semiconduct- ors. Nature Materials, 13(12), 1096-1101.

[11] Wang, G., Glazov, M. M., Robert, C., Amand, T., Marie, X. and Urbaszek, B. (2015). Double resonant Raman scattering and valley coherence generation in monolayer WSe_2. Physical Review Letters, 115(11), 117401.

[12] Li, T. and Galli, G. (2007). Electronic properties of MoS_2 nanoparticles. *The* Journal of Physical Chemistry C, 111(44), 16192-16196.

[13] Splendiani, A., Sun, L., Zhang, Y., Li, T., Kim, J., Chim, C. Y. and Wang, F. (2010). Emerging photoluminescence in monolayer MoS_2. Nano Letters, 10(4), 1271-1275.

[14] Zhao, W., Ribeiro, R. M., Toh, M., Carvalho, A., Kloc, C., Castro Neto, A. H. and Eda, G. (2013). Origin of indirect optical transitions in few-layer MoS_2, WS_2, and WSe_2. Nano Letters, 13(11), 5627-5634.

[15] Vidal, L. N. and Vazquez, P. A. Frequency dependent Raman scattering activities of BeH_2, MgH_2, CaH_2, SrH_2, and H_2O, H_2S, H_2Se, H_2Te, evaluated by the ab initio relativistic four component method Dirac–Hartree–Fock. Chemical physics, 2006, 321(1), 209-214.